Applied Catalysis B: Environment and Energy 344 (2024) 123623

Contents lists available at ScienceDirect

Applied Catalysis B: Environment and Energy

journal homepage: www.elsevier.com/locate/apcatb

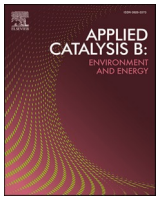

Gamma-valerolactone-enabled control chemoselective conversion of glucose to 1,6-anhydroglucose over HZSM-5 zeolite

Yao Liu [a], Qixuan Lin [a,*], Qiwen Zhan [a], Hui Zhang [a], Ruonan Zhu [a], Xingjie Wang [a], Libo Li [b], Junli Ren [a,*]

[a] State Key Laboratory of Pulp and Paper Engineering, School of Light Industry and Engineering, South China University of Technology, Guangzhou 510640, China
[b] School of Chemistry and Chemical Engineering, South China University of Technology, Guangzhou 510640, China

ARTICLE INFO

Keywords:
Glucose
Dehydration
Shape selective catalysis
γ-valerolactone
Biomass upgrading

ABSTRACT

Unraveling chemoselective catalysis in the upgrading of renewable biomass-derived molecules to fine chemicals and bio-fuels is particularly challenging. Here, we report an innovative strategy for the chemocatalytic conversion of glucose into 1,6-anhydroglucose, a high-value platform molecule, in γ-valerolactone (GVL) over HZSM-5 (50) zeolite. In this case, HZSM-5 (50) zeolite exhibits remarkable shape-selective catalytic performance with a high turn-over frequency (TOF) of 201.6 h^{-1} and a 1,6-anhydroglucose selectivity of 95.3%. Solvent effect study from both experimental and theoretical results suggests the usage of solvent GVL is particularly beneficial for glucose diffusion into the zeolite pore channel, accelerating the isomerization-dehydration process. Kinetic behavior description of glucose transformation to 1,6-anhydroglucose is developed to monitor the process, whereas a synergistic catalytic mechanism is elucidated in detail by density functional theory calculations. Such solvent-induce and shape-selective catalytic system provides a compelling strategy for highly selective production of 1,6-anhydroglucose as a biomass platform molecule.

1. Introduction

Catalytic upgrading of renewable lignocellulosic biomass to high value-added chemicals and liquid fuels is receiving ever increasing attention in view of mitigating the energy crisis and environmental concerns [1–3]. Glucose, derived from the chemical or biochemical hydrolysis of cellulose or starch, or even directly from lignocellulosic biomass [4,5], has been identified as the most abundant sugar platform to manufacture high-value chemicals through various reactions [6–10]. In particular, the selective conversion of glucose into 1,6-anhydroglucose (1,6-anhydro-β-D-glucopyranose (AGP) and 1,6-anhydro-β-D-glucofuranose (AGF)) has potential application value in biorefinery. Because 1,6-anhydroglucose is not only an important building-block chemical widely utilized in the synthesis of biodegradable surfactants, stereoregular polysaccharides, and hyperbranched polysaccharides [11–13], but also a molecular tracer for biomass burning in the environmental field [14–16].

Currently, 1,6-anhydroglucose is primarily produced by the pyrolysis of glucose and cellulose [13,17,18]. However, most of the pyrolysis processes suffer from their harsh conditions (high temperature and pressure), posing potential risks to security. What's worse, the low product selectivity and difficulty in target product separation largely limit their further practical application [19,20]. Due to the growing demand for 1,6-anhydroglucose, development of novel chemocatalytic processes is imperative to overcome above issues and boost 1,6-anhydroglucose production. Recently, due to their gentle required conditions and highly tunable nature in dehydration process during the glucose upgrading, catalytic dehydration has emerged as a more friendly strategy for the synthesis of valuable chemicals (e.g., 5-hydroxymethylfurfural, HMF) [21,22]. As such, it was then proposed that catalytic dehydration should uphold high potential to enhance the 1,6-anhydroglucose production in a similar reaction manner. In such a catalytic process, two major concerns need to be addressed, namely, catalyst design as well as solvent selection. Several studies have reported that regulating relative abundance and proximity of Lewis and Brønsted acid sites in the catalysts can affect the reactivity of glucose dehydration [6], and the solvent plays a significant role in influencing the product distribution and accumulation [23]. However, to the best of our knowledge, only Takagaki et al. [24] performed the catalytic dehydration investigation for glucose transformation to 1,6-anhydroglucose in *N*,

* Corresponding authors.
E-mail addresses: linqixuan@scut.edu.cn (Q. Lin), renjunli@scut.edu.cn (J. Ren).

https://doi.org/10.1016/j.apcatb.2023.123623
Received 12 October 2023; Received in revised form 6 December 2023; Accepted 14 December 2023
Available online 19 December 2023

N-dimethylformamide over a sulfonated solid acid catalyst (Amberlyst-15), obtaining 88% glucose conversion and 63% 1,6-anhydroglucose yield. Nevertheless, the catalytic selectivity still needs to be improved, and the detailed factors of solvent properties and catalytic mechanism have not yet been fully investigated. It should be specially pointed out that the selectivity of glucose dehydration reaction is usually insufficient because of the complex thermodynamic distributions of products in acidic media (Scheme 1) [25–27]. As such, selectivity control remains very challenging in the catalytic dehydration process [28,29]. In this respect, establishing an effective catalytic dehydration system for producing 1,6-anhydroglucose from glucose with high conversion and selectivity is highly desirable.

Enlightened by the above research situations, we have established a novel strategy for the selective catalytic dehydration of glucose to 1,6-anhydroglucose over HZSM-5 zeolite in γ-valerolactone (GVL, a green biobased solvent). This catalytic system exhibits excellent catalytic activity (TOF = 201.6 h^{-1}) and product yield (95.3%). Meanwhile, a high recycled stability of HZSM-5 (50) zeolite and GVL solvent is achieved by a simple separation strategy. More importantly, density functional theory (DFT) calculations and molecular dynamics (MD) simulation are used extensively to study the solvent effect and dehydration mechanism of glucose to 1,6-anhydroglucose in detail. Also, a kinetic model for the dehydration reaction of glucose to AGP and AGF is established to monitor the process. Subsequently, the underlying catalytic mechanism is also elaborated.

2. Experimental section

The details of the chemicals, catalyst activity tests, product analysis and catalyst characterization are provided in the Supporting Information, Text S1-S4. Prior to the product analysis, 10 mL of water was added to the reaction mixture at the end of the reaction to dissolve sugar compounds due to the fact that glucose is not completely soluble in GVL at room temperature (Fig. S1). The HZSM-5 zeolite model system for density functional theory (DFT) calculations and Molecular dynamics (MD) simulation is shown in Fig. 1, and the details computational method are described in the Supporting Information, Text S5.

3. Results and discussion

3.1. Catalytic behavior evaluation of various catalysts

Initially, the catalytic behavior of commercially available heterogeneous catalysts (metal oxides, acidic resin, heteropoly acid, and H-form zeolites) for glucose reaction in GVL was investigated, and the results are summarized in Table 1. Extremely weak dehydration activity, with a glucose conversion of only 10.8% at 190 °C for 20 min, is found when no catalyst was used (entry 1, Table 1). For all catalytic cases, the glucose conversion is in the range of 24.8–100%, with the turnover frequency (TOF) being in the range of 68.6–245.9 h^{-1} (entries 2–11, Table 1). Among them, H-form zeolites (Hβ, HY, H-MOR, and HZSM-5 (Si/Al=30, 50 and 80)) exhibit excellent catalytic activity (TOF > 102.6 h^{-1}) and high 1,6-anhydroglucose formation rate (15.0–47.6 mmol/g·h^{-1}) (entry 6–11, Table 1). Although the usage of Al_2O_3, Amberlyst-15 and $H_3PW_{12}O_{40}$ also results in high glucose conversion, their main products are fructose (2.1–23.5% yield), HMF (0–25.3% yield) and FAL (0–11.0% yield) with low 1,6-anhydroglucose yield (0–17.5%) (entries 3–5, Table 1). Notably, H-form zeolites possess a higher BET surface area and smaller pore diameter than that of the other tested heterogeneous catalysts (Fig. S2 and Table S1), and displayed a visible catalytic selectivity. The systematic investigations reveal that the porous properties play a critical role in the catalytic conversion process (Fig. S3). In particular, HZSM-5 (50) zeolite, which had appropriate porous properties (S_{BET} = 238 $m^2 \cdot g^{-1}$, D_{pore} = 4.15 nm, and V_{pore} = 0.07 $cm^3 \cdot g^{-1}$) (Table S1), afforded complete consumption of glucose and a near quantitative selectivity of 1,6-anhydroglucose (95.3%) (entry 10, Table 1). The remarkable catalytic activity and selectivity can be ascribed to the shape-selective catalysis of HZSM-5 (50) zeolite (Fig. S3) [30]. Comparatively, the HZSM-5 (Si/Al=30 and 80) with similar framework structure showed distinctly dropped catalytic performances for 1,6-anhydroglucose production (entries 9–11, Table 1 and Table S1). The dramatic differences in the selectivity among these HZSM-5 suggested that the better catalytic performance of HZSM-5 (50) zeolite catalysis relies not only on the unique textural properties of the zeolite framework but also on the local active sites [31].

To unveil the structure-active site relationship of the catalyst and its catalytic behavior, the acid properties of the H-form zeolites were investigated by NH_3-TPD and Py-FTIR. In Fig. 2a, all H-form zeolites exhibited two obvious desorption peaks of NH_3 in the range of 50–250 °C and 300–550 °C, ascribing to the weak and moderate acidic sites, respectively [32,33]. While HY and HZSM-5(80) zeolites also showed a third peak, representing the presence of strong acidic sites (around 600–800 °C). Based on the quantitative analysis of NH_3-TPD, the total acid amounts of acid sites in H-form zeolites were calculated to be in the range of 0.65–2.07 mmol/g. Apparently, the total acid amount in HZSM-5 zeolites was gradually decreased with the increase of the Si/Al ratio from 30 to 80, which can be ascribed to the loss of weak and moderate acidic sites. Combined with the results shown in Table 1, no clear intrinsic correlation was found between the total acid amount and the catalytic behaviors. To be specific, HZSM-5 (50) zeolite exhibited the highest catalytic selectivity among all HZSM-5 zeolites, however its total acid amount sits in the middle among all three catalysts (2.07, 0.93 and 0.65 mmol/g for HZSM-5 (30), HZSM-5 (50), and HZSM-5 (80) zeolites, respectively). It is worth mentioning that glucose catalytic conversion is a classical acid-driven reaction, while acid sites, such as Brønsted and Lewis acid, are critically active for the synthesis of valuable chemicals [6,8].

To investigate the role of the acidic properties of the H-form zeolites,

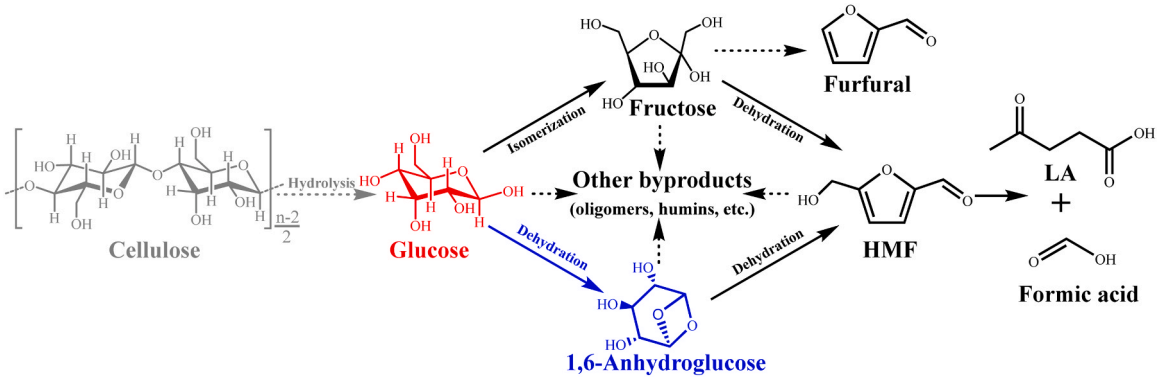

Scheme 1. Catalytic conversion of glucose to 1,6-anhydroglucose and other fine chemicals in acidic media.

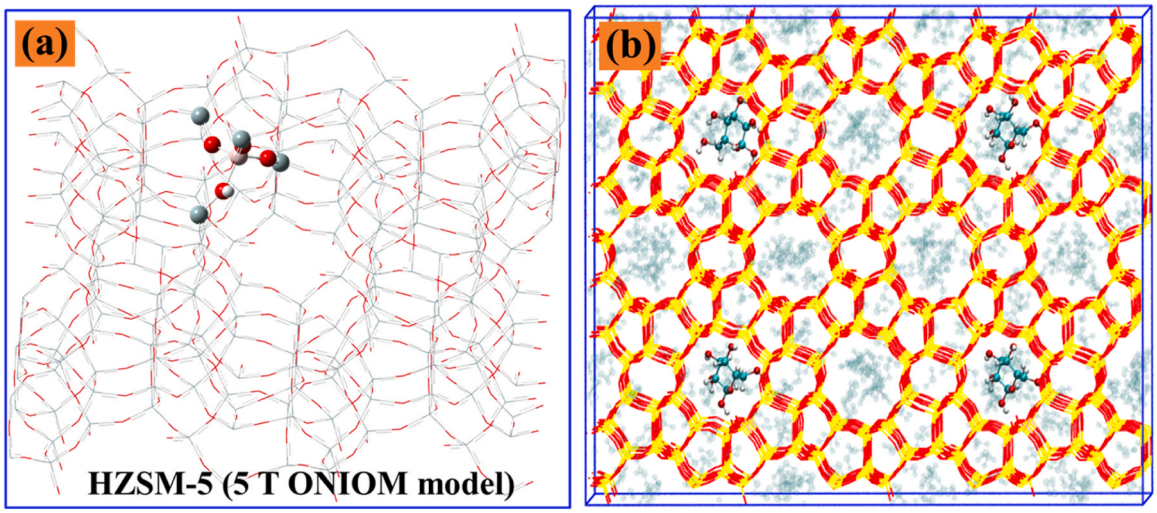

Fig. 1. HZSM-5 zeolite model system: (a) 5 T ONIOM model. The high layer atoms (ball and stick) are calculated with the M06–2X/6–311 + G(d,p), while the low layer atoms (wire frame) are calculated with UFF, (b) MD calculation model. Four glucose molecules are inserted into the supercell, and then filled with solvent molecules (green).

Table 1
Catalytic dehydration of glucose over various catalysts.

Entry	Catalyst	Conv. %	Yield %					Selec. %	Y_{rate} $mmol \cdot g^{-1} \cdot h^{-1}$	TOF h^{-1}	C.B. %
			AGP	AGF	Fru	HMF	FAL				
1	Blank	10.8	6.5	2.7	-	-	-	85.2	-	-	85.2
2	ZrO_2	24.8	5.0	2.2	14.7	-	-	29.0	3.6	103.2	88.3
3	Al_2O_3	86.5	8.2	5.1	23.5	-	-	15.4	6.6	77.2	42.5
4	Amberlyst-15	> 99.9	12.3	5.2	3.9	25.3	7.0	17.5	8.8	68.6	53.7
5	$H_3PW_{12}O_{40}$	> 99.9	-	-	2.1	-	11.0	-	-	78.0	13.1
6	Hβ	> 99.9	22.7	7.5	3.0	5.2	9.7	30.2	15.0	153.0	48.1
7	HY	> 99.9	39.8	12.0	2.1	8.8	4.7	51.8	25.9	109.4	67.4
8	H-MOR	95.6	57.0	16.9	1.6	-	-	77.3	36.9	102.6	79.0
9	HZSM-5(30)	> 99.9	63.9	18.3	-	-	-	82.2	41.1	140.3	82.2
10	HZSM-5(50)	> 99.9	72.5	22.8	-	-	-	95.3	47.6	201.6	95.3
11	HZSM-5(80)	> 99.9	56.0	16.1	-	-	-	72.1	36.1	245.9	72.1

Note: Reaction conditions: glucose, 0.3 g; GVL, 20 mL; HZSM-5 (50), 0.1 g; temperature, 190 °C; time, 20 min. The formation rate of 1,6-anhydroglucose (Y_{rate}) = (mmoles of formed 1,6-anhydroglucose)/(catalyst amount × time), turnover frequency (TOF) = (moles of converted glucose)/(mass of catalyst used × acid amount × time) and carbon balance (C.B.) = yield of liquid products (AGP, AGF, Fru, HMF and FAL)/glucose conversion.

the Brønsted and Lewis acid sites were further analyzed by Py-FTIR. As shown in Fig. 2b, the bands at 1446 and 1595 cm^{-1} are ascribed to pyridine adsorbed on Lewis acid sites, 1546 cm^{-1} is attributed to pyridine adsorbed on Brønsted acid sites and 1489 cm^{-1} is designated as pyridine adsorbed on both Lewis and Brønsted acid sites [2,34]. According to the quantitative analysis of Py-FTIR, the number of Lewis acid sites in Hβ, HY, and H-MOR zeolites (186.5–284.58 μmol/g) is markedly higher than that of HZSM-5 zeolites (20.09–135.55 μmol/g). The more Lewis acid sites have been identified to facilitate the isomerization of glucose to fructose and subsequent dehydration to HMF (Scheme 1) [25,35]. In our catalytic tests, fructose was indeed detected during the reaction for Hβ, HY, and H-MOR zeolites, leading to the decreasing selectivity of 1,6-anhydroglucose (Table 1). However, among the tested HZSM-5 zeolites, HZSM-5 (50) zeolite, possessing a lower amount of Lewis acid site than HZSM-5 (30) zeolite (135.55 μmol/g) but a higher Lewis acid site (59.36 μmol/g) than that of HZSM-5 (80) zeolite (20.09 μmol/g), emerged as the most selective catalyst. The result suggests that the Lewis acid site significantly influences the distribution of the products, with high Lewis acid sites contributing to the formation of fructose. It is known that that the Brønsted acid site can be responsible for catalyzing the dehydration of glucose [6,22]. Fig. 2c shows that the synergistic catalysis of Lewis and Brønsted acid site is the key to the selective preparation of 1,6-anhydroglucose. Obviously, with the Lewis and Brønsted acid sites in the range of 50–120 and 40–90 μmol/g, respectively, as well as the relative equilibrium of Brønsted and Lewis acid sites (B/L≈1), a high 1,6-anhydroglucose yield can be achieved. Additionally, high Brønsted acid site is not conducive to high 1,6-anhydroglucose yield, because the excessive Brønsted acid sites can drive the undesirable reaction, resulting in the decomposition of glucose and 1,6-anhydroglucose into by-products [36,37]. From the above analysis, it can be derived that the proper acid amount and the suitable ratio between Lewis and Brønsted acid sites facilitates the selective conversion of glucose to 1,6-anhydroglucose.

3.2. Solvent effect on the glucose conversion and product yields

To gain more insights into the solvent-mediated interactions during the production of 1,6-anhydroglucose over HZSM-5(50) zeolite, both experiments and computations were performed to study the solvent effect. As indicated in Table 2, it presented the lowest dehydration reactivity when water was used as the reacting solvent, with the TOF of 7.3 h^{-1} and 1,6-anhydroglucose formation rate of 2.0 $mmol \cdot g^{-1} \cdot h^{-1}$. Prominently, a highest yield of 1,6-anhydroglucose (95.3%) was achieved in the presence of GVL compared to other solvents. When

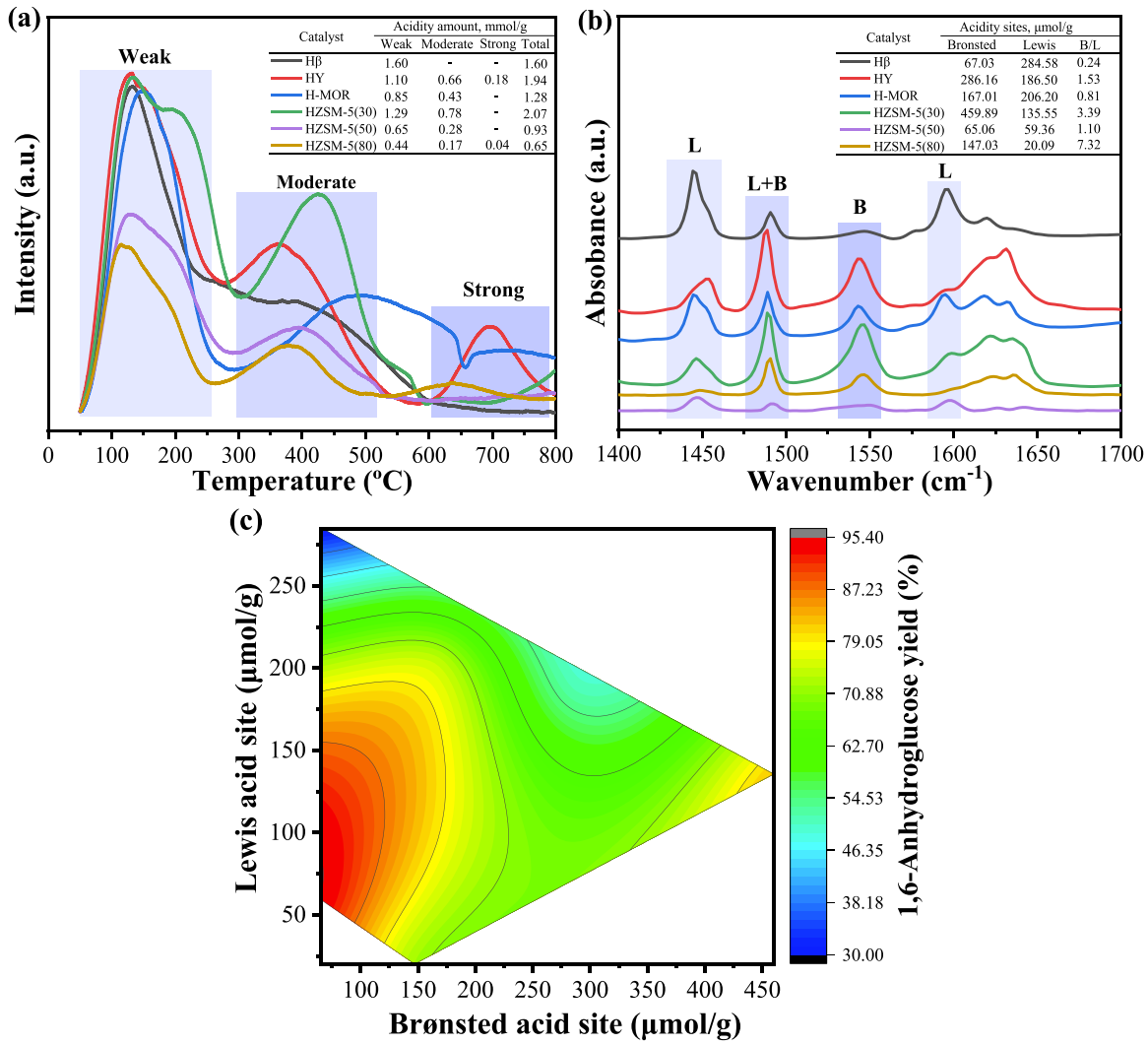

Fig. 2. NH_3-TPD (a) and Py-FTIR (b) results of various H-form zeolites, and the color-contour chart of 1,6-anhydroglucose yield as a function of Brønsted acid site and Lewis acid site (c).

Table 2
Screening of various solvents for glucose conversion.

Entry	Solvent	Conv. %	Yield %					Selec. %	Y_{rate} mmol·g^{-1}·h^{-1}	TOF h^{-1}	C.B. %
			AGP	AGF	Fru	HMF	FAL				
1	H_2O	13.5	2.5	1.5	10.0	-	-	29.6	2.0	7.3	> 99.9
2	Methanol	48.8	1.0	3.6	34.3	-	-	9.4	2.3	26.2	79.7
3	GVL	> 99.9	72.5	22.8	-	-	-	95.3	47.6	201.6	95.3
4	MIBK	73.7	6.1	2.5	0.8	-	-	11.7	4.3	39.6	12.8
5	DMF	45.0	2.7	1.6	13.8	-	-	9.6	2.2	24.2	40.2
6	DMSO	87.0	35.9	24.8	2.2	7.6	-	69.8	30.3	46.7	81.0
7	MeTHF	65.9	3.9	2.2	1.9	-	-	9.2	3.1	35.4	12.1

Note: Reaction conditions: glucose, 0.3 g; solvent, 20 mL; HZSM-5 (50), 0.1 g; temperature, 190 °C; time, 20 min

methanol, MIBK, DMF, DMSO, and MeTHF were used as solvents, the reaction suffered from low chemoselectivity, which can be due to the ease of by-product (such as fructose, HMF and especially humins) generation [2,38]. Moreover, it is noted that HMF was only detected in the reaction where DMSO was applied as the solvent. As presented in Table S3, the conversion of glucose is less than 31.9% in different solvents without any addition of catalyst, and their 1,6-anhydroglucose yields are not satisfied. In brief, different types of solvent can regulate the reaction equilibrium and thus the product distribution. GVL is conducive to the enhancing reactivity and the restraining occurrence of side reactions.

DFT and MD calculations were applied to investigate the influence of actual solvent environment on the production of 1,6-anhydroglucose over HZSM-5(50) zeolite. As depicted in Table S2, the solvation free energy (ΔG_{sol}) of glucose (including glucopyranose and glucofuranose) increases in the following order: water < methanol < GVL < MIBK < DMF < DMSO < MeTHF. In general, low ΔG_{sol} is favorable for glucose solubilization, followed by easy access to the active site of the HZSM-5 (50) zeolite and accelerates the reaction in catalytic process [39]. Unexpectedly, the catalytic activity was relatively low in water and

methanol (TOF < 26.2 h^{-1}), although both medium displayed the lowest ΔG_{sol}. Furthermore, the ΔG_{sol} value in GVL was the third smallest among all tested solvents, achieving a 100% of glucose conversion (TOF = 201.6 h^{-1}). These results implied that the ΔG_{sol} value is not the only determinant factor affecting the catalytic conversion of glucose. On the other hand, the energy barriers of glucopyranose were all lower than those of glucofuranose in different solvents (Fig. 3a), indicating glucopyranose is easier to form during tautomeric equilibrium, which also led to the higher yield of AGP than AGF (Table 1 and Table 2).

It is worth mentioning that fructose is a by-product in this work derived from the isomerization of glucose, and its formation relies on the usage of Lewis acidic and/or basic catalyst and alkaline medium[40,41]. Interestingly, the results indicated that solvents also significantly affected the fructose formation, and 0–34.4% of fructose yield was obtained over HZSM-5 (50) zeolite in various solvents (Table 2). We thus speculate that the alkaline strength of solvent plays an extremely crucial role in influencing the highly selective conversion of glucose to 1, 6-anhydroglucose and alleviating the formation of fructose. To assess this, quantum chemical calculations were performed to calculate the proton affinity using as the basicity of solvent (Fig. 3b). It could be clearly observed that DMSO has the strongest proton affinity (ΔE_{pa} = 891.77 kJ/mol), followed by DMF, MeTHF, GVL, MIBK, methanol and water. The strong ΔE_{pa} will induce the isomerization-dehydration reaction of glucose and ultimately mediate the formation of HMF [2,38]. This result further explained the phenomenon that HMF was only produced in the presence of DMSO. Among the solvents tested, GVL has a relatively weak proton affinity (ΔE_{pa} = 832.57 kJ/mol) and exhibits the highest catalytic selectivity. This result was due to weak basicity can promote the isomerization of glucose to intermediate (*INT*), and selectively produced 1,6-anhydroglucose, which will be discussed in detail later in the MD calculations. On the other hand, water and methanol have the weakest proton affinity (ΔE_{pa} < 750.13 kJ/mol), but fructose was obtained as the main product with yields of 10.0% and 34.3%, respectively, resulting in low 1,6-anhydroglucose selectivity. This was mainly attributed to the lowest ΔG_{sol} value of water and methanol (Table S2), which made it easier for glucose to contact with the Lewis acid site of the HZSM-5 (50) and isomerized to produce fructose [26].

The accessibility of different solvents within the internal pores of the zeolite catalyst has a variability that affects internal diffusion of glucose into the catalyst pore channel. Through the MD simulation, the result indicates that the order of interaction energy (E_{sc}) for solvent diffusion into the pore channel of the HZSM-5(50) zeolite follows as below: DMF < DMSO < GVL < MeTHF < Methanol < MIBK < H_2O (Table 3). The smaller the E_{sc} will result in a stronger attraction between the solvent and the zeolite pore channel, making it easier for the solvent to penetrate into the pore channels. Therefore, when the DMF/DMSO/GVL is used as the medium, glucose can diffuse easily into the internal pore channel of the HZSM-5 zeolite for reaction. At the same time, the isomerization reaction will occur after glucose enters the catalyst pore channel and approaches the active site. During the glucose

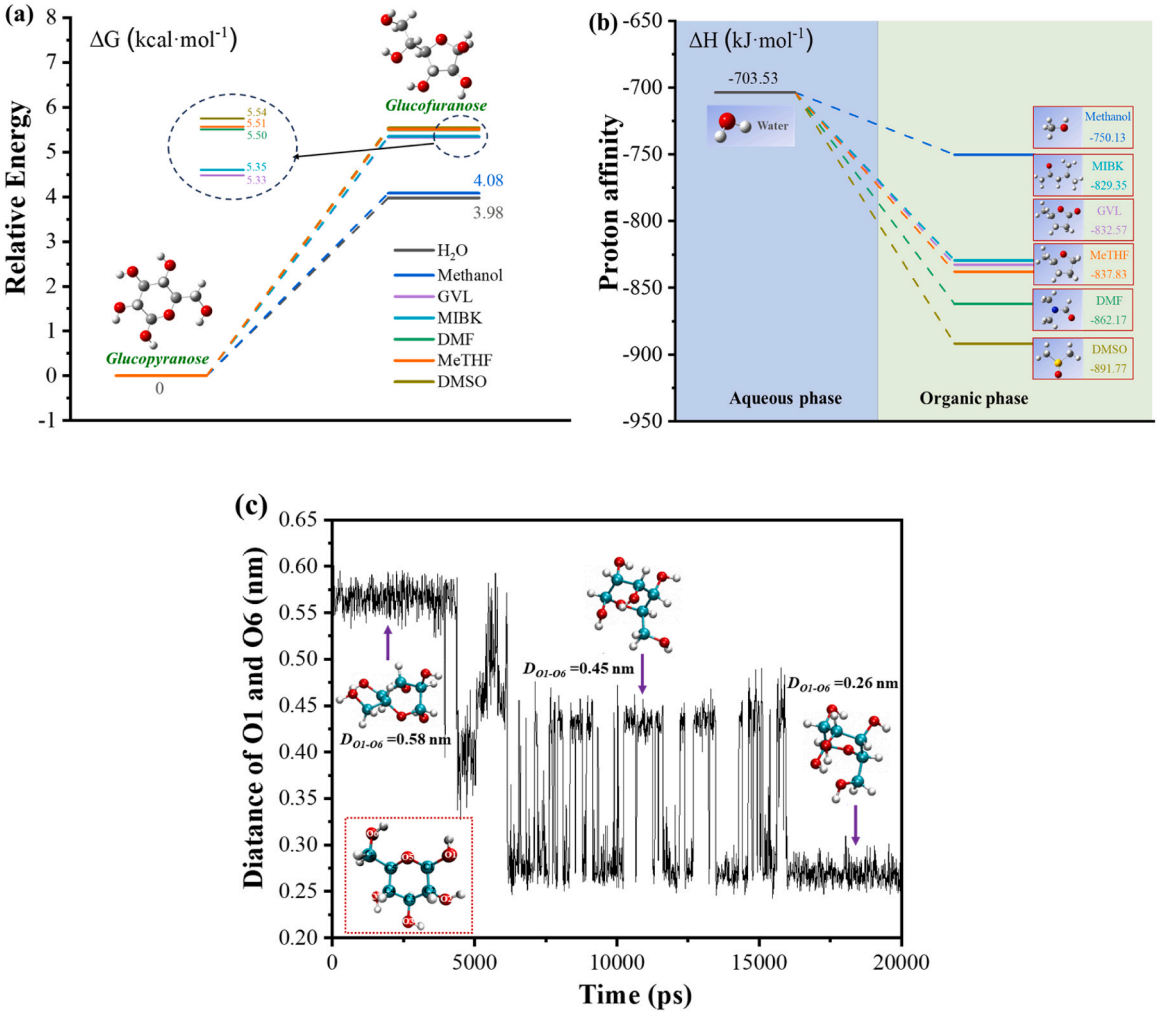

Fig. 3. The energy barrier diagrams of the glucopyranose and glucofuranose in different solvents (a), the basicity of solvents calculated as the proton affinity (b) and the variations of O1-O6 distances in glucose with time (c).

Table 3
The interaction energy and the average proportion of configurations with $D_{O1\text{-}O6}$ less than 0.35 nm.

entry	solvent	E_{sc}, kcal/mol	Average proportion of configuration ($D_{O1\text{-}O6}$ < 0.35 nm), %
1	H_2O	-2286.48	25.50
2	Methanol	-2888.78	0
3	GVL	-4090.84	21.49
4	MIBK	-2862.66	10.28
5	DMF	-4456.94	0.21
6	DMSO	-4410.17	15.98
7	MeTHF	-3939.62	2.05

isomerization process, we computationally observed three main isomeric conformations, the O1-O6 distances ($D_{O1\text{-}O6}$) of which are 0.58, 0.45 and 0.26 nm (Fig. 3c). Among them, the conformation ($D_{O1\text{-}O6}$ =0.26 nm) is beneficial for the efficient production of 1,6-anhydroglucose, and detailed catalytic mechanism is discussed in following study. Therefore, we performed calculations of the average proportion of configurations with $D_{O1\text{-}O6}$ less than 0.35 nm in different solvents, and the results are summarized in Table 3. The detailed variation of O1-O6 distances in four glucose is given in Fig. S4. It is noticeable that the H_2O/GVL/DMSO is particularly beneficial for the formation of configuration with $D_{O1\text{-}O6}$ less than 0.35 nm compared to the other tested solvents (methanol, MIBK, DMF and MeTHF). Combined with the E_{sc} results, it can be found that although water exhibits a conformational advantage (25.50%), its poor accessibility to the catalyst pore channel results in the inability to obtain 1,6-anhydroglucose in high yield. Whereas DMF easily brings glucose into the catalyst pore channel, the conformation (0.21%) is not favorable for the formation of the target product. Comparatively, GVL and DMSO possess conformational advantages and low interaction energies, thus enabling high yield of 1,6-anhydroglucose. However, the higher alkalinity of DMSO promotes the production of HMF from glucose, resulting in a decrease in 1,6-anhydroglucose yield.

As stated above, the solvents' nature affects their presenting properties including solubilization, diffusion and isomerization, resulting in different product distribution during the glucose conversion reaction (Fig. S5). The low ΔG_{sol} value will be beneficial for glucose solubilization and facilitate its access to the active site (Lewis acid) of HZSM-5 (50), thus significantly increasing the isomerization of glucose to fructose. The strong ΔE_{pa} will also facilitate the isomerization of glucose, which will then be further converted to HMF. Moreover, the small E_{sc} plays a significant role in driving glucose into the pore channel of the HZSM-5 zeolite, facilitating the subsequent shape-selective isomerization of glucose into intermediates. GVL has the appropriate properties (including ΔG_{sol}, E_{sc}, ΔE_{pa} and average proportion of configuration, $D_{O1\text{-}O6}$ < 0.35 nm), which significantly affect the weak isomerization of glucose to intermediate, and further highly selective dehydration to 1,6-anhydroglucose.

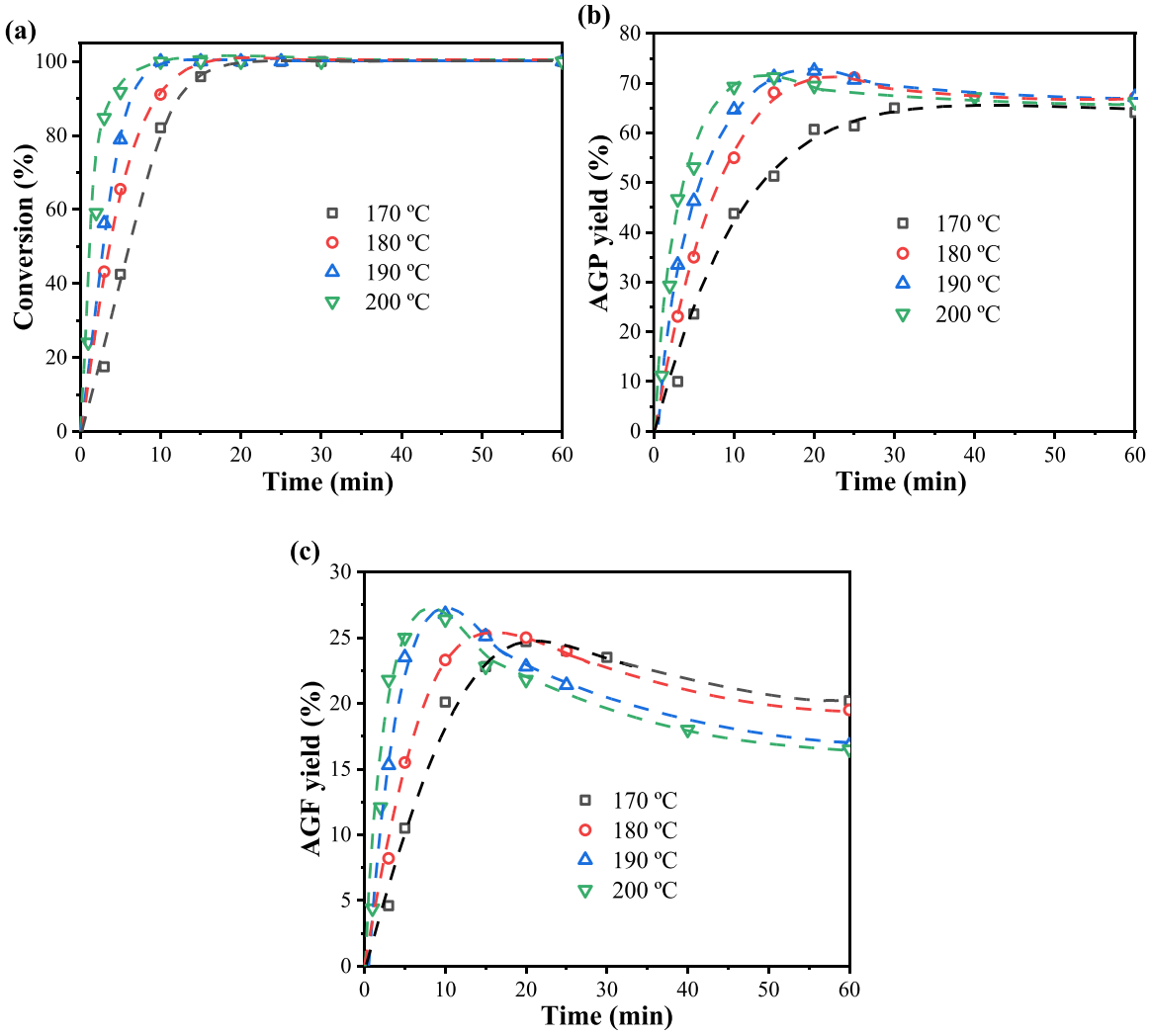

Fig. 4. Effect of reaction temperature and time on the catalytic conversion of glucose: glucose conversion (a), AGP yield (b) and AGF yield (c).

3.3. Kinetic study

To further reveal the reaction network of glucose conversion in GVL over HZSM-5 (50), the kinetic behavior was investigated in the temperature range of 170–200 °C. As shown in Fig. 4, the glucose conversion remarkably elevates as the temperature increase and 100% conversion can be reached within 10 min when the reaction was run at 200 °C. While the yield of AGP and AGF also see their increase in the initial stage. Obviously, the reaction time also has a similar influence trend to that of the temperature. However, as the temperature and time overstepped the corresponding critical values, AGP and AGF yield decreased, possibly due to the occurrence of side reactions such as the undetectable and undissolved polymeric products. Furthermore, the yield of AGP decreased significantly less than that of AGF, indicating that AGP is more stable in the catalytic system. Based on the above results, a simplified kinetic model was applied to assess the intrinsic catalytic activity of HZSM-5 (50) zeolite (Fig. 5), and the kinetic model was assumed to be a pseudo-first-order reaction, as follows:

$$\frac{dC_{glu}}{dt} = -(k_1 + k_2)C_{glu} \quad (1)$$

$$\frac{dC_{AGP}}{dt} = k_1 C_{glu} - k_3 C_{AGP} \quad (2)$$

$$\frac{dC_{AGF}}{dt} = k_2 C_{glu} - k_4 C_{AGF} \quad (3)$$

$$\frac{dC_{other}}{dt} = k_3 C_{AGP} + k_4 C_{AGF} \quad (4)$$

where k_i (i = 1, 2, 3, 4) is the reaction rate constant. C_{glu}, C_{AGP}, C_{AGF} and C_{other} are the real-time concentrations of glucose, AGP, AGF and other products, respectively.

The experimental results of catalytic dehydration of glucose were then fitted to these equations to obtain the reaction rate constant. As depicted in Fig. S6, a good correlation ($R^2 > 0.95$) was obtained between the predicted and measured data, revealing the robustness of this kinetic model. The reaction rate constants of the glucose dehydration network are shown in Fig. 6. It was observed that the formation-rate of AGP is faster than that of AGF, with the k_1 value being 2-fold higher than k_2. A contrary trend is observed for the side reactions, and the value of k_4 is one of magnitude larger than that of k_3. This indicated that the degradation rate of AGF is faster than that of AGP.

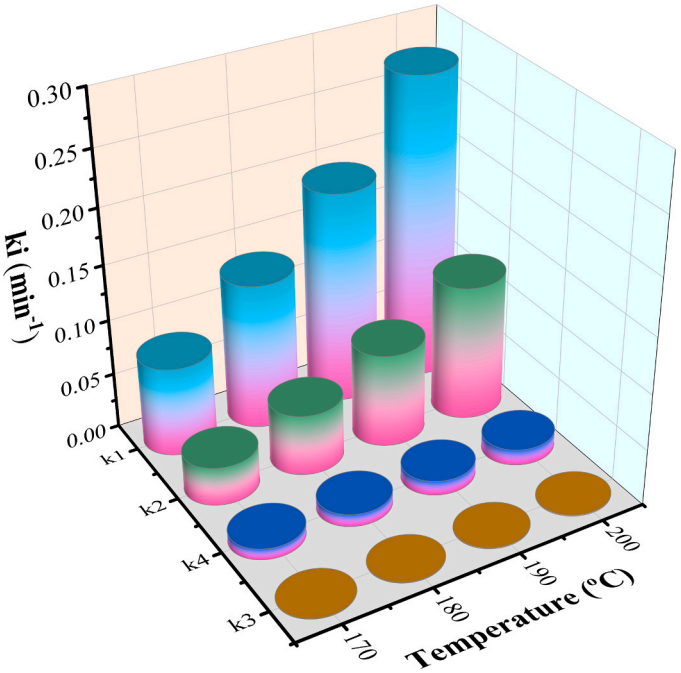

Fig. 6. Reaction rate constants of glucose dehydration network at different temperatures.

From the Arrhenius law, the apparent activation energy (E_i) of glucose dehydration network was calculated, and the results are shown in Fig. S7. The apparent activation energies of E_1, E_2, E_3 and E_4 were 70.7, 73.3, 38.3 and 21.4 kJ/mol, respectively. Interestingly, the activation energy (E_1) of glucopyranose dehydration was calculated to be 70.7 kJ/mol, which is lower than of the glucofuranose dehydration (E_2 =73.3 kJ/mol), revealing that the AGP is easier to generate during glucose dehydration process. In addition, it is noted that the activation energies of E_3 and E_4 are lower than those of E_1 and E_2, respectively, indicating that the degradation reactions of AGP and AGF are prone to

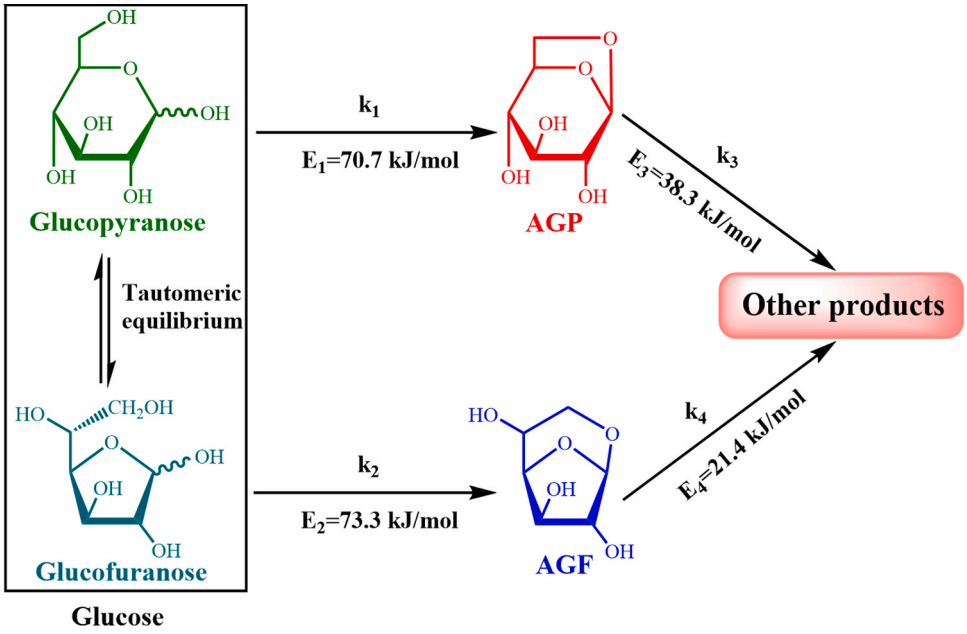

Fig. 5. Kinetic model of the catalytic conversion of glucose to AGP and AGF.

occur. Nevertheless, the generation rates of AGP and AGF (k_1 and k_2) are much faster than their degradation rates (k_3 and k_4) (Fig. 6), especially AGP degradation (k_3). This implies that 1,6-anhydroglucose can be selectively produced by modulating the reaction time and temperature. The established kinetic model is an effective tool for monitoring the dehydration process of glucose on HZSM-5(50), as well as for selective regulation to obtain the target product.

3.4. Reaction mechanism studies

In view of these observations, the catalytic conversion of glucose to AGP and AGF pertains to a bridging dehydration reaction [42]. Fig. 7 shows an underlying reaction mechanism for the selective conversion of glucose (including glucopyranose and glucofuranose) in the absence of a catalyst, and corresponding free energies for each step are calculated based on DFT. As shown in Fig. 7a, uncatalyzed dehydration of glucose generates AGP and AGF through a four-membered ring transition state (*Mechanism 1*). Taking glucopyranose dehydration as an example, two possible reaction paths (*TS1α* and *TS1β*) can be found for glucopyranose dehydration, including O1-H···H and O6-H···H dissociation (Fig. 7a and Fig. S8). Among them, the activation Gibbs energy ($\Delta G^{\ddagger}$) for the *TS1β* path is 56.75 kcal·mol^{-1}, which is lower than that for the *TS1α* path ($\Delta G^{\ddagger}$ = 80.23 kcal·mol^{-1}) (Fig. 7b). Similar results (*TS2β* < *TS2α*) can be found in the dehydration of glucofuranose (Fig. 7c). These results strongly demonstrate that the *TS1β* and *TS2β* path (O1-H···H dissociation) is more favorable in the absence of catalyst. Importantly, a low energy barrier for the *TS1β* path ($\Delta G^{\ddagger}$ = 56.75 kcal·mol^{-1}) was observed compared to that for the *TS2β* path ($\Delta G^{\ddagger}$ = 73.30 kcal·mol^{-1}), which indicates that the *TS1β* path is a preferential path for the generation of 1, 6-anhydroglucose (AGP), consistent with the experimental results (Table 1 and Table 2). In the following, we will only discuss the reaction mechanism of glucopyranose dehydration (O1-H···H dissociation) over the HZSM-5 (50) zeolite catalyst.

As mentioned above, Brønsted and Lewis acid sites on HZSM-5 zeolite catalyst mediate dehydration process and facilitate the highly selective dehydration of glucose to 1,6-anhydroglucose. While the Brønsted acid site (proton) in HZSM-5 zeolite is located in four nearly equivalent oxygen sites around the aluminum atom, caused by the substitution of aluminum for framework silicon, the aluminum atom is the Lewis acid site [36,43]. That is to say, the amount of Brønsted and Lewis acid sites in HZSM-5 zeolite is influenced by the framework Si/Al ratio. Fig. 8a depicts the proposed mechanism for the conversion of glucopyranose to AGP on HZSM-5 zeolite (*Mechanism 2*). The proton

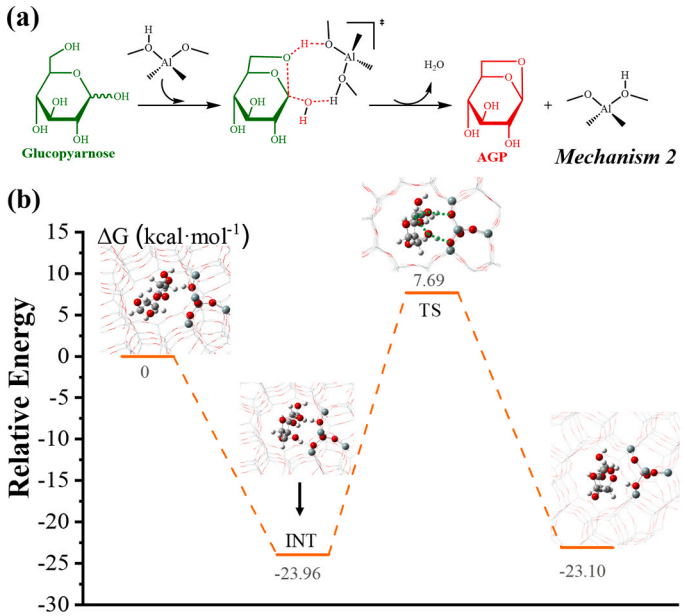

Fig. 8. Proposed mechanisms for the conversion glucopyranose into APG on HZSM-5 zeolite in GVL (a) and the corresponding reaction energy diagrams (b).

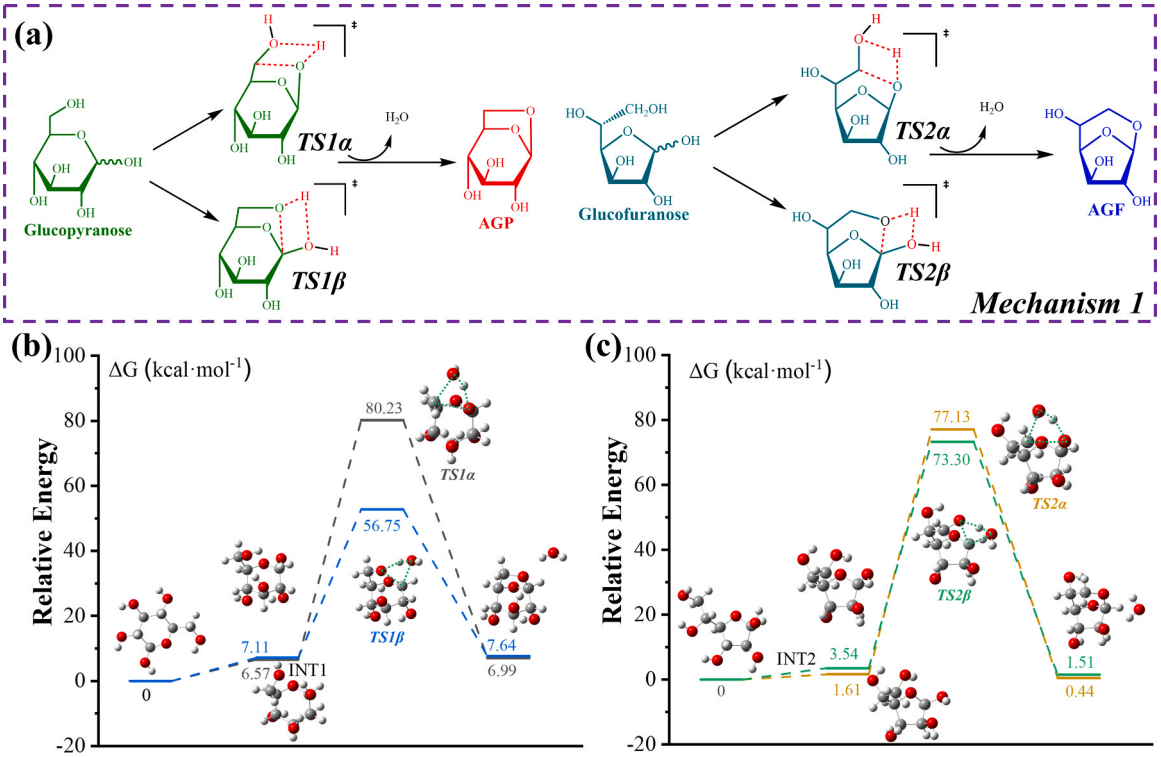

Fig. 7. Proposed mechanisms for the conversion glucose into APG and AGF in the absence of catalyst in GVL: Mechanism1 (a), and the reaction energy diagrams for the dehydration of glucopyranose (b) and glucofuranose (c).

transfers from the HZSM-5 Brønsted acidic site (Al-(OH)-Si) to the glucopyranose (O1-H) are concurrent with water dissociation, and the proton on glucopyranose O6 is transferred to an adjacent oxygen atom of the zeolite framework (Al−O−Si). This transformation proceeds via the formation of an eight-membered ring transition state (*TS*). As expected, the DFT calculation indicates a significant reduction of the activation Gibbs energy ($\Delta G^{\ddagger}$ = 31.65 kcal·mol^{-1}) for the conversion of glucopyranose to AGP in the presence of HZSM-5 zeolite (Fig. 8b). In all calculated cases, the O1-H and O6-H atoms of glucopyranose are first activated and isomerized to intermediate (*INT*) with an O1-O6 distance of 2.52 Å (Fig. S9), which is a key reaction process for the highly selective production of AGP. In our catalytic system, the small number of Lewis acid sites in the HZSM-5 (50) zeolite, as well as the weak alkaline strength of GVL, contributed to the smooth isomerization of glucose to *INT* and reduced the activation Gibbs energy of the reaction.

3.5. Reusability test of HZSM-5 (50) zeolite and GVL

The reusability of the HZSM-5 (50) catalyst and GVL solvent for the glucose dehydration was evaluated for five runs under optimal conditions (190 °C, 20 min). As depicted in Fig. 9a, the resulting reaction mixtures can be separated by a simple procedure to obtain post-catalysis HZSM-5 (50) zeolite and chemicals. Upon completion of the separation process, the as-obtained recycled HZSM-5 (50) zeolite and recovered GVL solvent were employed for the next cycle directly under the identical reaction conditions. As expected, the target product 1,6-anhydroglucose can be obtained with a purity of 96.0%, which is also further determined by GC-MS (Fig. S10). Excitedly, the catalytic activity of recycled HZSM-5 (50) zeolite remained almost the same after five runs, and the glucose conversion and 1,6-anhydroglucose yield can achieved 100% and 93.2%, respectively (Fig. 9b). This confirms that HZSM-5 (50) zeolite possesses excellent catalytic durability and recyclability toward the dehydration of glucose to 1,6-anhydroglucose. The reusability of GVL solvent on glucose conversion is further evaluated (Fig. 9c). After 5 runs, the glucose conversion (92.7%) and 1,6-anhydroglucose yield (86.0%) decreased slightly compared to the first run using fresh GVL solvent. This is due to the fact that the recovered GVL solvent is not pure and a small amount of by-products (e.g., water) will accumulate after five successive runs, which is not conducive to glucose dehydration [36]. In a word, the designed catalytic system is developed as a vigorous route for the efficient conversion of glucose to 1,6-anhydroglucose with high selectivity, and the catalyst and solvent can be easily separated and reused for more than 5 times.

4. Conclusions

In summary, we developed a simple and highly efficient catalytic strategy for the conversion of glucose into 1,6-anhydroglucose in GVL solution. HZSM-5 (50), which integrates both weak Brønsted and Lewis acid sites, exhibits a remarkable shape-selective catalytic performance in transformation of glucose to 1,6-anhydroglucose with a quantitative conversion (100%) and 95.3% selectivity. Systematic experimental studies and theoretical calculations reveal that the solvent GVL in the catalytic system plays multiple vital roles: 1) dissolve the glucose and assist its diffusion into the HZSM-5 (50) zeolite pore channels, 2) cooperate with Lewis acid sites to promote glucose isomerization to intermediate and thus enhance the overall catalytic selectivity. The kinetic studies indicated that the AGP formation process is endowed with

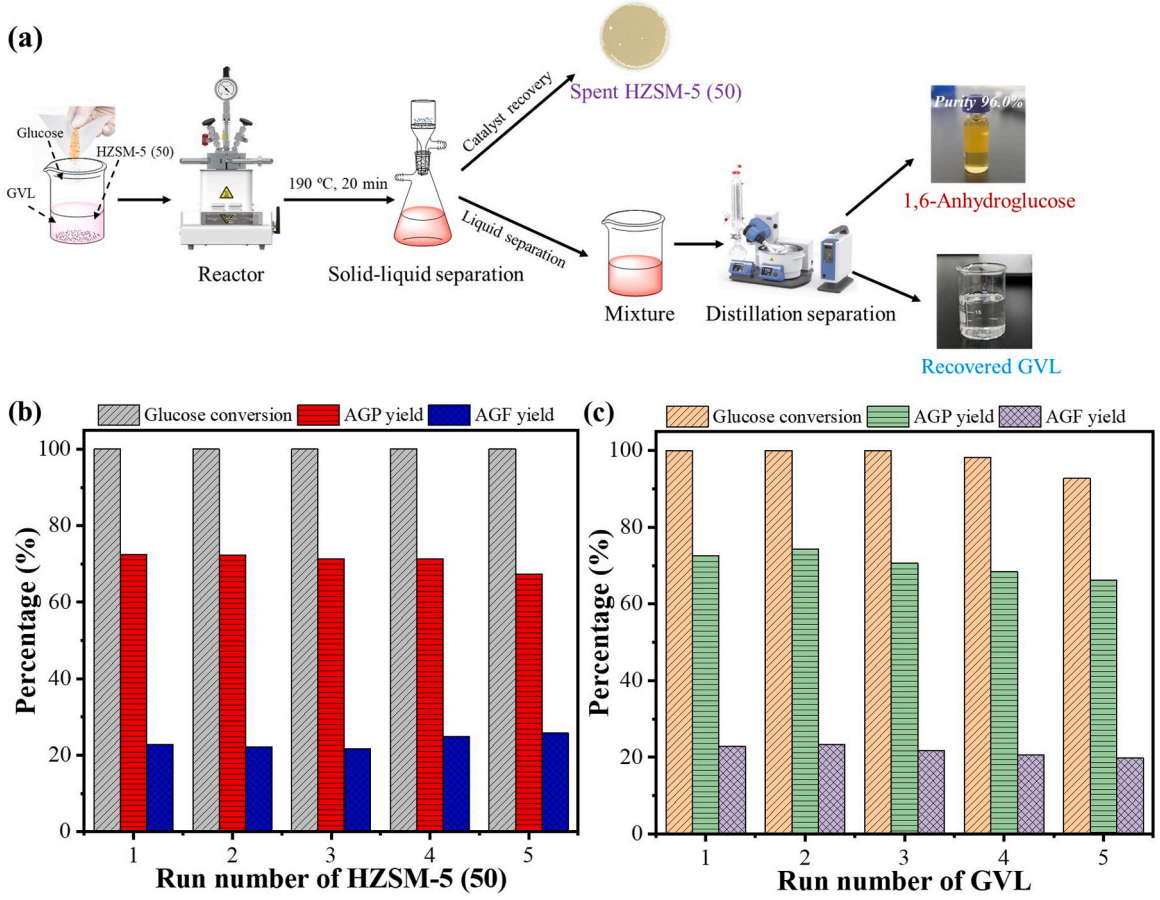

Fig. 9. The separation procedure of the chemicals from the reaction mixture (a), and the reusability test of the HZSM-5 (50) catalyst (b) and GVL solvent (c) in the conversion of glucose. Reaction conditions: glucose, 0.3 g; GVL, 20 mL; HZSM-5 (50), 0.1 g; temperature, 190 °C; time, 20 min.

the high reaction rate constant k_1 and low degradation rate constant k_3, as well as relatively low apparent activation energy E_1. The reaction mechanism for dehydration of glucose to 1,6-anhydroglucose was provided in detail by DFT computations, demonstrating glucose O1-H•••H dissociation is the most favorable path, and a low activation Gibbs energy for catalytic dehydration significantly accelerates the selective formation of 1,6-anhydroglucose. Further, the HZSM-5 (50) zeolite and GVL solvent could be easily recovered and reused at least five times with no distinct changes in activity. This work will provide inspiration for the future design of solvent-induce and shape-selective catalytic systems for highly selective dehydration processes in biomass-derived molecules.

CRediT authorship contribution statement

Zhu Ruonan: Funding acquisition, Investigation, Methodology, Project administration, Resources, Validation. **Wang Xingjie:** Formal analysis, Funding acquisition, Validation, Writing – original draft, Writing – review & editing. **Ren junli:** Funding acquisition, Investigation, Methodology, Project administration, Resources, Supervision, Validation, Writing – review & editing. **Li Libo:** Methodology, Resources, Software. **Liu Yao:** Conceptualization, Data curation, Formal analysis, Investigation, Methodology, Writing – original draft, Writing – review & editing, Software. **Lin Qixuan:** Conceptualization, Data curation, Formal analysis, Funding acquisition, Software, Writing – original draft. **Zhan Qiwen:** Investigation, Methodology, Project administration, Writing – review & editing. **Zhang Hui:** Investigation, Methodology, Resources, Software, Writing – review & editing.

Declaration of Competing Interest

The authors declare that they have no known competing financial interests or personal relationships that could have appeared to influence the work reported in this paper.

Data availability

Data will be made available on request.

Acknowledgements

This work described in this paper was financially supported by National Natural Science Foundation of China (Nos. 22178135, 22208113), China Postdoctoral Science Foundation (Pre-Station) (No. 2023TQ0121), Guangzhou Municipal Science and Technology Bureau (No. 202201010386), State Key Laboratory of Pulp and Paper Engineering (No. 202303) and the Fundamental Research Funds for the Central Universities of SCUT, China (No.2022ZYGXZR106).

Appendix A. Supporting information

Supplementary data associated with this article can be found in the online version at doi:10.1016/j.apcatb.2023.123623.

References

[1] M.J. Zeng, X.J. Pan, Insights into solid acid catalysts for efficient cellulose hydrolysis to glucose: progress, challenges, and future opportunities, Catal. Rev. Sci. Eng. 64 (2022) 445–490, https://doi.org/10.1080/01614940.2020.1819936.
[2] R. Li, Q.X. Lin, J.L. Ren, Z.H. Guo, Y.X. Wang, X.B. Yang, X.J. Wang, Insights into the synergistic effect of catalyst acidity and solvent basicity for effective production of pentose from glucose, Chem. Eng. J. 442 (2022), 136224, https://doi.org/10.1016/j.cej.2022.136224.
[3] Y.J. Shen, Q.S. Zheng, H.B. Zhu, T. Tu, Hierarchical porous organometallic polymers fabricated by direct knitting: recyclable single-site catalysts with enhanced activity, Adv. Mater. 32 (2020), 1905950, https://doi.org/10.1002/adma.201905950.
[4] Q.Y. Liu, S. Luo, W. Fan, X.P. Ouyang, X.Q. Qiu, Separation of short-chain glucan oligomers from molten salt hydrate and hydrolysis to glucose, Green. Chem. 23 (2021) 4114–4124, https://doi.org/10.1039/d1gc00851j.
[5] L. Hu, L. Lin, Z. Wu, S.Y. Zhou, S.J. Liu, Chemocatalytic hydrolysis of cellulose into glucose over solid acid catalysts, Appl. Catal. B-Environ. 174 (2015) 225–243, https://doi.org/10.1016/j.apcatb.2015.03.003.
[6] W.Z. Guo, T. Kortenbach, W. Qi, E. Hensen, H.J. Heeres, J. Yue, Selective tandem catalysis for the synthesis of 5-hydroxymethylfurfural from glucose over in-situ phosphated titania catalysts: insights into structure, bi-functionality and performance in flow microreactors, Appl. Catal. B-Environ. 301 (2022), 120800, https://doi.org/10.1016/j.apcatb.2021.120800.
[7] B. Cai, J.F. Feng, D.Y. Guo, S. Wang, T.Y. Ma, T.L. Eberhardt, H. Pan, Highly efficient isomerization of glucose to fructose over a novel aluminum doped graphitic carbon nitride bifunctional catalyst, J. Clean. Prod. 346 (2022), 131144, https://doi.org/10.1016/j.jclepro.2022.131144.
[8] G.K. Beh, C.T. Wang, K. Kim, J.T. Qu, J. Cairney, Y.H. Ng, A.K. An, R. Ryoo, A. Urakawa, W.Y. Teoh, Flame-made amorphous solid acids with tunable acidity for the aqueous conversion of glucose to levulinic acid, Green. Chem. 22 (2020) 688–698, https://doi.org/10.1039/c9gc02567g.
[9] Z.F. Yan, J. Lian, Y. Feng, M.T. Li, F. Long, R.Q. Cheng, S. Shi, H. Guo, J.J. Lu, A mechanistic insight into glucose conversion in subcritical water: complex reaction network and the effects of acid-base catalysis, Fuel 289 (2021), 119969, https://doi.org/10.1016/j.fuel.2020.119969.
[10] Y. Ding, Y.Y. Cao, D.D. Chen, J. Li, H.G. Wu, Y. Meng, J.S. Huang, J.F. Yuan, Y. Q. Su, J.Q. Wang, H. Li, Relay photo/thermal catalysis enables efficient cascade upgrading of sugars to lactic acid: mechanism study and life cycle assessment, Chem. Eng. J. 452 (2023), 139687, https://doi.org/10.1016/j.cej.2022.139687.
[11] I. Itabaiana, M.A. do Nascimento, R. de Souza, A. Dufour, R. Wojcieszak, Levoglucosan: a promising platform molecule? Green. Chem. 22 (2020) 5859–5880, https://doi.org/10.1039/d0gc01490g.
[12] K. Wu, H. Wu, H.Y. Zhang, B. Zhang, C.Y. Wen, C.S. Hu, C. Liu, Q.Y. Liu, Enhancing levoglucosan production from waste biomass pyrolysis by Fenton pretreatment, Waste Manag. 108 (2020) 70–77, https://doi.org/10.1016/j.wasman.2020.04.023.
[13] S.S. Choi, M.C. Kim, Y.K. Kim, Influence of silica on formation of levoglucosan from carbohydrates by pyrolysis, J. Anal. Appl. Pyrolysis 90 (2011) 56–62, https://doi.org/10.1016/j.jaap.2010.10.009.
[14] C.Y. Lai, Y.C. Liu, J.Z. Ma, Q.X. Ma, H. He, Degradation kinetics of levoglucosan initiated by hydroxyl radical under different environmental conditions, Atmos. Environ. 91 (2014) 32–39, https://doi.org/10.1016/j.atmosenv.2014.03.054.
[15] Y.M. Li, T.M. Fu, J.Z. Yu, X. Feng, L.J. Zhang, J. Chen, S.K.R. Boreddy, K. Kawamura, P.Q. Fu, X. Yang, L. Zhu, Z.Z. Zeng, Impacts of chemical degradation on the global budget of atmospheric levoglucosan and its use as a biomass burning tracer, Environ. Sci. Technol. 55 (2021) 5525–5536, https://doi.org/10.1021/acs.est.0c07313.
[16] I.G. Hakeem, P. Halder, M.H. Marzbali, S. Patel, S. Kundu, J. Paz-Ferreiro, A. Surapaneni, K. Shah, Research progress on levoglucosan production via pyrolysis of lignocellulosic biomass and its effective recovery from bio-oil, J. Environ. Chem. Eng. 9 (2021), 105614, https://doi.org/10.1016/j.jece.2021.105614.
[17] X.L. Zhang, W.H. Yang, C.Q. Dong, Levoglucosan formation mechanisms during cellulose pyrolysis, J. Anal. Appl. Pyrolysis 104 (2013) 19–27, https://doi.org/10.1016/j.jaap.2013.09.015.
[18] T. Hosoya, S. Sakaki, Levoglucosan formation from crystalline cellulose: importance of a hydrogen bonding network in the reaction, Chemsuschem 6 (2013) 2356–2368, https://doi.org/10.1002/cssc.201300338.
[19] M.S. Mettler, A.D. Paulsen, D.G. Vlachos, P.J. Dauenhauer, The chain length effect in pyrolysis: bridging the gap between glucose and cellulose, Green. Chem. 14 (2012) 1284–1288, https://doi.org/10.1039/c2gc35184f.
[20] Z.G. Yang, X.P. Liu, Z.D. Yang, G.Q. Zhuang, Z.H. Bai, H.X. Zhang, Y.F. Guo, Preparation and formation mechanism of levoglucosan from starch using a tubular furnace pyrolysis reactor, J. Anal. Appl. Pyrolysis 102 (2013) 83–88, https://doi.org/10.1016/j.jaap.2013.03.012.
[21] N.A.S. Ramli, N.A.S. Amin, Fe/HY zeolite as an effective catalyst for levulinic acid production from glucose: characterization and catalytic performance, Appl. Catal. B-Environ. 163 (2015) 487–498, https://doi.org/10.1016/j.apcatb.2014.08.031.
[22] Q.D. Hou, M.N. Zhen, L. Liu, Y. Chen, F. Huang, S.Q. Zhang, W.Z. Li, M.T. Ju, Tin phosphate as a heterogeneous catalyst for efficient dehydration of glucose into 5-hydroxymethylfurfural in ionic liquid, Appl. Catal. B-Environ. 224 (2018) 183–193, https://doi.org/10.1016/j.apcatb.2017.09.049.
[23] Y.Q. Wang, G.Q. Ding, X.H. Yang, H.Y. Zheng, Y.L. Zhu, Y.W. Li, Selectively convert fructose to furfural or hydroxymethylfurfural on Beta zeolite: the manipulation of solvent effects, Appl. Catal. B-Environ. 235 (2018) 150–157, https://doi.org/10.1016/j.apcatb.2018.04.043.
[24] A. Takagaki, K. Ebitani, Glucose to Value-added chemicals: anhydroglucose formation by selective dehydration over solid acid catalysts, Chem. Lett. 38 (2009) 650–651, https://doi.org/10.1246/cl.2009.650.
[25] C.E. Bounoukta, C. Megias-Sayago, F. Ammari, S. Ivanova, A. Monzon, M. A. Centeno, J.A. Odriozola, Dehydration of glucose to 5-Hydroxymethlyfurfural on bifunctional carbon catalysts, Appl. Catal. B-Environ. 286 (2021), 119938, https://doi.org/10.1016/j.apcatb.2021.119938.
[26] H.G. Zhang, H. Zhao, S.X. Zhai, R.X. Zhao, J. Wang, X. Cheng, H.S. Shiran, S. Larter, M.G. Kibria, J.G. Hu, Electron-enriched Lewis acid-base sites on red carbon nitride for simultaneous hydrogen production and glucose isomerization, Appl. Catal. B-Environ. 316 (2022), 121647, https://doi.org/10.1016/j.apcatb.2022.121647.
[27] F.H. Richter, K. Pupovac, R. Palkovits, F. Schuth, Set of acidic resin catalysts to correlate structure and reactivity in fructose conversion to 5-hydroxymethylfurfural, Acs Catal. 3 (2013) 123–127, https://doi.org/10.1021/cs3007439.

[28] M.A. Mellmer, C. Sanpitakseree, B. Demir, P. Bai, K.W. Ma, M. Neurock, J. A. Dumesic, Solvent-enabled control of reactivity for liquid-phase reactions of biomass-derived compounds, Nat. Catal. 1 (2018) 199–207, https://doi.org/10.1038/s41929-018-0027-3.
[29] D. Wu, W.Y. Hernandez, S.W. Zhang, E.I. Vovk, X.H. Zhou, Y. Yang, A. Y. Khodakov, V.V. Ordomsky, In situ generation of bronsted acidity in the Pd-I bifunctional catalysts for selective reductive etherification of carbonyl compounds under mild conditions, Acs Catal. 9 (2019) 2940–2948, https://doi.org/10.1021/acscatal.8b04925.
[30] T.L. Cui, W.Y. Ke, W.B. Zhang, H.H. Wang, X.H. Li, J.S. Chen, Encapsulating palladium nanoparticles inside mesoporous MFI zeolite nanocrystals for shape-selective catalysis, Angew. Chem. Int. Ed. 55 (2016) 9178–9182, https://doi.org/10.1002/anie.201602429.
[31] Z.P. Hu, G.Q. Qin, J.F. Han, W.N. Zhang, N. Wang, Y.J. Zheng, Q.K. Jiang, T. Ji, Z. Y. Yuan, J.P. Xiao, Y.X. Wei, Z.M. Liu, Atomic insight into the local structure and microenvironment of isolated Co-motifs in MFI zeolite frameworks for propane dehydrogenation, J. Am. Chem. Soc. 144 (2022) 12127–12137, https://doi.org/10.1021/jacs.2c02636.
[32] J.N. Wei, T. Wang, X.J. Cao, H. Liu, X. Tang, Y. Sun, X.H. Zeng, T.Z. Lei, S.J. Liu, L. Lin, A flexible Cu-based catalyst system for the transformation of fructose to furanyl ethers as potential bio-fuels, Appl. Catal. B-Environ. 258 (2019), 117793, https://doi.org/10.1016/j.apcatb.2019.117793.
[33] H.P. Winoto, Z.A. Fikri, J.M. Ha, Y.K. Park, H. Lee, D.J. Suh, J. Jae, Heteropolyacid supported on Zr-Beta zeolite as an active catalyst for one-pot transformation of furfural to gamma-valerolactone, Appl. Catal. B-Environ. 241 (2019) 588–597, https://doi.org/10.1016/j.apcatb.2018.09.031.
[34] J.H. Zhang, Y. Liu, S.B. Yang, J.N. Wei, L. He, L.C. Peng, X. Tang, Y.H. Ni, Highly selective conversion of furfural to furfural alcohol or levulinate ester in one pot over ZrO_2@SBA-15 and its kinetic behavior, Acs Sustain. Chem. Eng. 8 (2020) 5584–5594, https://doi.org/10.1021/acssuschemeng.9b07512.
[35] Q. Yang, S.F. Zhou, T. Runge, Magnetically separable base catalysts for isomerization of glucose to fructose, J. Catal. 330 (2015) 474–484, https://doi.org/10.1016/j.jcat.2015.08.008.
[36] W.P. Song, H. Liu, Y. Sun, J.H. Zhang, L.C. Peng, Understanding Hβ zeolite in 1,4-dioxane efficiently converts hemicellulose-related sugars to furfural, Acs Catal. 12 (2022) 12833–12844, https://doi.org/10.1021/acscatal.2c03227.
[37] H. Nguyen, N. Xiao, S. Daniels, N. Marcella, J. Timoshenko, A. Frenkel, D. G. Vlachos, Role of lewis and bronsted acidity in metal chloride catalysis in organic media: reductive etherification of furanics, Acs Catal. 7 (2017) 7363–7370, https://doi.org/10.1021/acscatal.7b02348.
[38] M. Asakawa, A. Shrotri, H. Kobayashi, A. Fukuoka, Solvent basicity controlled deformylation for the formation of furfural from glucose and fructose, Green. Chem. 21 (2019) 6146–6153, https://doi.org/10.1039/c9gc02600b.
[39] Q.X. Lin, Q.W. Zhan, R. Li, S.W. Liao, J.L. Ren, F. Peng, L.B. Li, Solvent effect on xylose-to-furfural reaction in biphasic systems: combined experiments with theoretical calculations, Green. Chem. 23 (2021) 8510–8518, https://doi.org/10.1039/d1gc02812j.
[40] J. Wang, H. Zhao, B.C. Zhu, S. Larter, S.W. Cao, J.G. Yu, M.G. Kibria, J.G. Hu, Solar-driven glucose isomerization into fructose via transient lewis acid-base active sites, Acs Catal. 11 (2021) 12170–12178, https://doi.org/10.1021/acscatal.1c03252.
[41] K. Karádi, T.T. Nguyen, A.A. Adám, K. Baán, A. Sápi, A. Kukovecz, Z. Kónya, P. Sipos, I. Pálinkó, G. Varga, Structure-activity relationships of LDH catalysts for the glucose-to-fructose isomerisation in ethanol, Green. Chem. 25 (2023) 5741–5755, https://doi.org/10.1039/d3gc01860a.
[42] B. Hu, Q. Lu, X.Y. Jiang, J. Liu, M.S. Cui, C.Q. Dong, Y.P. Yang, Formation mechanism of hydroxyacetone in glucose pyrolysis: a combined experimental and theoretical study, Proc. Combust. Inst. 37 (2019) 2741–2748, https://doi.org/10.1016/j.proci.2018.05.146.
[43] S. Kim, D.J. Robichaud, G.T. Beckham, R.S. Paton, M.R. Nimlos, Ethanol dehydration in HZSM-5 studied by density functional theory: evidence for a concerted process, J. Phys. Chem. A 119 (2015) 3604–3614, https://doi.org/10.1021/jp513024z.